Indonesian Journal of Pharmacy

VOL 34 (4) 2023: 630–639 | RESEARCH ARTICLE

Study of 1-Formyl-2-Pyrazolines as Anticancer Drug Candidates

Artania Adnin Tri Suma[1*] and Tutik Dwi Wahyuningsih[2]

1. Department of Pharmaceutical Chemistry, Faculty of Pharmacy, Universitas Gadjah Mada, Sekip Utara, Bulaksumur, Yogyakarta, 55281, Indonesia.
2. Department of Chemistry, Faculty of Mathematics and Natural Sciences, Universitas Gadjah Mada, Sekip Utara, Bulaksumur, Yogyakarta, 55281, Indonesia.

Article Info

Submitted: 11-03-2023
Revised: 14-09-2023
Accepted: 12-10-2023

*Corresponding author
Artania Adnin Tri Suma

Email:
artania.adnin.t.s@ugm.ac.id

ABSTRACT

The development of novel anticancer agents is essential in cancer prevention. One versatile group of compounds, known for their significant bioactivity and several of its derivatives that have been clinically approved, is the group of pyrazolines. This study aimed to synthesize 1-formyl-2-pyrazoline derivatives (pyrazolines **1-2**) using chalcone **1-2**, hydrazine hydrate, and formic acid via cyclo-condensation. The synthesized compounds were characterized using Fourier Transform Infrared (FTIR), Gas Chromatography-Mass Spectrometry (GC-MS), and Nuclear Magnetic Resonance (^{1}H- and ^{13}C-NMR) spectrometers. Pyrazolines **1-2** were found to be drug-like compounds, satisfying Lipinski's Rule of Five and possessing favorable absorption, distribution, metabolism, and excretion (ADME) properties, including good gastrointestinal absorption, blood-brain barrier permeability, and no interaction with P-glycoprotein. Furthermore, they were inactive against several toxicity endpoints in a normal body condition, such as immunotoxicity, mutagenicity, and cytotoxicity. *In vitro* cytotoxic evaluation of the pyrazolines **1-2** against HeLa and MCF7 cancer cell lines demonstrated moderate activity, with IC_{50} values of 25.01 µM and 82.87 µM, respectively. Pyrazolines **1-2** also showed good selectivity with selectivity index (SI) values of 8.92 and 14.45. The molecular docking study on epidermal growth factor receptor tyrosine kinase (EGFR-TK) (PDB ID: 4HJO) revealed that pyrazolines **1-2** had a binding affinity of -7.9 and -8.0 kcal/mol, respectively. The compounds interacted with Lys721 residue through hydrogen bonds and hydrophobic interactions due to the presence of the pyrazoline ring and the formyl group in their structures. These findings suggest that pyrazolines **1-2** scaffold has the potential to be further studied as a lead compound for anticancer drug candidates.

Keywords: pyrazoline, anticancer, synthesis, docking, ADMET

INTRODUCTION

Cancer is a disease caused by the uncontrollable growth of abnormal or damaged cells, slowly spreading and invading other parts of the body (Upadhyay, 2021). It is a leading cause of death worldwide, with its incidence and mortality rates increasing rapidly (Brennan & Davey-Smith, 2022). In 2020, an estimated 19.3 million new cases and 10 million deaths were recorded globally (Sung *et al*., 2021). The development of novel anticancer agents with high efficacy and low toxicity is crucial in preventing cancer (Zhong *et al*., 2021). Heterocyclic compounds play a significant role in medicinal chemistry, while pyrazoline, a five-membered nitrogen-containing heterocycle, is a versatile compound used in developing novel anticancer agents (Matiadis & Sagnou, 2020; Lang *et al*., 2020). The 1-substituted-2-pyrazolines that contain various functional groups have been shown to enhance their bioactivity (Karabacak *et al*., 2015; Mustofa *et al*., 2022; Rana *et al*., 2022). Several pyrazoline-bearing drugs are clinically approved and used for various medical conditions, including some that act as tyrosine kinase inhibitors in anticancer therapy. For example, Ibrutinib (Imbruvica) is used for chronic lymphocytic leukemia and Mantle cell lymphoma, and Axitinib (Inlyta) is a medication for severe aplastic anemia and refractory aplastic anemia (Haider *et al*., 2022; Nehra *et al*., 2020).

Copyright © 2023 by Indonesian Journal of Pharmacy (IJP). The open access articles are distributed under the terms and conditions of Creative Commons Attribution 2.0 Generic License (https://creativecommons.org/licenses/by/2.0/).

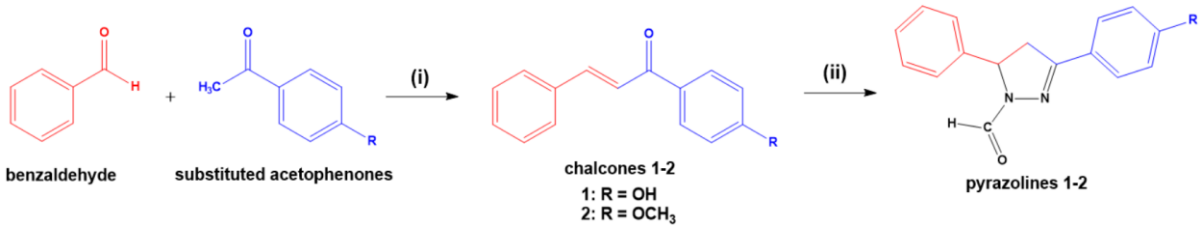

Figure 1. Synthesis of 1-formyl-2-pyrazolines. Reagents and conditions: (i) 40% KOH, MeOH, sonication, Troom; (ii) NH_2NH_2, HCOOH, 30% NaOH, EtOH, reflux.

There are various methods of synthesizing pyrazoline derivatives, depending on the source of the nitrogen and carbon atoms in the pyrazoline ring. The nitrogen atoms are typically derived from specific reactants such as hydrazines, diazoalkanes, and nitrilimines (Matiadis, 2023). Hydrazines are frequently used as the reactant since they can provide two nitrogen atoms in the pyrazoline ring. In this synthetic route, hydrazines are reacted with α,β-enones in the presence of an acid catalyst to produce the desired pyrazolines (Vahedpour *et al*., 2021). Furthermore, *in silico* analysis has proven helpful in predicting a proposed compound's molecular mechanism of action with a receptor (Rashid *et al*., 2021).

This research aimed to synthesize and examine the anticancer activity of formyl-substituted pyrazolines **1-2** (Figure 1). A study reported the potential of pyrazoline **2** as a xanthine oxidase inhibitor (Joshi *et al*., 2021). However, further investigation on pyrazoline **2** as an anticancer has not been reported yet, as well as pyrazoline **1**. Therefore, in this study, the drug properties and interaction of pyrazolines **1-2** were assessed via drug-likeness prediction using Lipinski's rule of five, pharmacokinetic study by ADMET (absorption, distribution, metabolism, excretion, toxicity) prediction, and molecular docking study. Moreover, *in vitro* testing was performed to evaluate the cytotoxicity of the pyrazolines against various cancer cell lines such as WiDr (colorectal cancer), HeLa (cervical cancer), MCF7, T47D, and 4T1 (breast cancer). Pyrazolines **1-2** were synthesized through a two-step process. First, the α,β-enones were prepared via Claisen-Schmidt condensation reaction between methoxy- and hydroxy-substituted acetophenones with benzaldehyde. Second, the α,β-enones were subjected to a cyclo-condensation reaction with hydrazines in the presence of formic acid.

MATERIALS AND METHODS

Materials and Instruments

The chemicals used for the synthesis procedures in this study were analytical grade from Merck, namely 4-hydroxyacetophenone, 4-methoxyacetophenone, benzaldehyde, hydrazine hydrate, formic acid, methanol, ethanol, montmorillonite, potassium hydroxide, sodium hydroxide, hydrochloric acid (37%), *n*-hexane, and ethyl acetate. The progress of the reaction was monitored using thin-layer chromatography, an aluminum plate coated with silica gel 60 F254 from Merck. Cytotoxicity was accessed using cancer cell lines (WiDr, HeLa, MCF7, T47D, 4T1), non-malignant cell lines (Vero), Dulbecco's Modified Eagle Medium (DMEM) solution, Roswell Park Memorial Institute Medium (RPMI 1640) solution, Medium 199 (M199) solution, dimethylsulfoxide, Fetal Bovine Serum (FBS) solution, penicillin-streptomycin solution, trypsin-EDTA solution, phosphate buffer solution, 3-(4,5-dimethylthiazol-2-yl)-2,5-diphenyltetrazolium bromide (MTT) solution, and sodium dodecyl sulfate (SDS) solution.

The determination of melting points was performed using Electrothermal 9100. The structure elucidation of all compounds was performed using Shimadzu Prestige-21 using KBr discs to obtain infrared (IR) spectra, Shimadzu QP2010S (electron ionization) to get gas chromatography (GC) chromatogram and mass spectra, and JEOL JNMECA (500 MHz and 125 MHz) to obtain proton and carbon nuclear magnetic resonance (^{1}H- and ^{13}C-NMR) spectra. The cytotoxicity evaluation was carried out using 96-microwell plates (Biologix), micropipette (VWR and AccuBioTech), incubator (Heraeus), inverted microscope (Axiovert25), and ELISA reader (BIO-RAD Benchmark).

Synthesis Procedures

Synthesis of (*E*)-1-(4-hydroxyphenyl)-3-phenylprop-2-en-1-one (Chalcone 1)

Chalcone **1-2** were synthesized based on literature (Suma *et al*., 2019) with some modifications. A solution of 0.68 g (5 mmol) of 4-hydroxyacetophenone and 0.53 g (5 mmol) of benzaldehyde in 10 mL of methanol was prepared. The mixture was then added with 0.10 g of montmorillonite and 10 mL of 40% (w/v) KOH solution, and the mixture was sonicated for 3 h at room temperature. The reaction mixture was then cooled by adding ice and 10% (v/v) HCl solution until it reached pH 2. After refrigerating for 24 hours, the resulting precipitate was filtered, washed with cold water, and dried under a vacuum. Recrystallization was performed to obtain the solid white product with a yield of 89.28%, a purity of 100% by GC-MS, a melting point of 178 °C, and an Rf value of 0.17 (*n*-hexane:ethyl acetate, 4:1, v/v). Mass spectrum (EI), m/z: 224 (M^+). FTIR spectrum (KBr), ν_{max} (cm^{-1}): 3132 (O–H str.), 1605 (C=O str.), 1580 and 1512 (aromatic C=C str.), 980 (*trans* =C–H bend.). ^{1}H-NMR (500 MHz), δ (ppm): 6.87 (2H, *d*, J = 8.5 Hz, ArH), 7.39-7.41 (3H, *m*, ArH), 7.70 (1H, *d*, J = 13.5 Hz, *trans* =CH_α), 7.71-7.74 (2H, *m*, ArH), 7.73 (1H, *d*, J = 14.0 Hz, *trans* =CH_β), 7.77 (1H, *s*, O–H) 8.01 (2H, *d*, J = 8.5 Hz, ArH). ^{13}C-NMR (125 MHz), δ (ppm): 116.48 (2C, ArH), 123.02 (1C, C_α), 123.35 (2C, ArH), 130.15 (2C, ArH), 130.95 (1C, ArH), 131.63 (2C, ArH), 133.06 (1C, Ar), 136.06 (1C, Ar), 145.23 (1C, C_β), 164.16 (1C, ArOH), 190.06 (1C, C=O).

Synthesis of (*E*)-1-(4-methoxyphenyl)-3-phenylprop-2-en-1-one (Chalcone 2)

A total of 0.75 g (5 mmol) 4-methoxycetophenone and 0.53 g (5 mmol) benzaldehyde were diluted in 10 mL of methanol. The mixture was then added with 10 mL of 40% (w/v) KOH solution. After sonicating the mixture at room temperature for 3 h and performing the same working-up procedure for chalcone **1,** the resulting solid was purified through recrystallization. This process yielded a yellowish-white solid in 89.07%, with a purity of 100% by GC-MS, a melting point of 106 °C, and an Rf value of 0.52 (*n*-hexane:ethyl acetate, 3:1, v/v). Mass spectrum (EI), m/z: 238 (M^+). FTIR spectrum (KBr), ν_{max} (cm^{-1}): 1605 (C=O str.), 1570 and 1496 (aromatic C=C str.), 1257 (C–O str.), 972 (*trans* =C–H bend.). ^{1}H-NMR (500 MHz), δ (ppm): 3.86 (3H, *s*, –OCH_3), 6.97 (2H, *d*, J = 8.5 Hz, ArH), 7.39-7.41 (3H, *m*, ArH), 7.55 (1H, *d*, J = 15.5 Hz, *trans* =CH_α), 7.62-7.63 (2H, *m*, ArH), 7.78 (1H, *d*, J = 16.0 Hz, *trans* =CH_β), 8.03 (2H, *d*, J = 9.0 Hz, ArH). ^{13}C-NMR (125 MHz), δ (ppm): 55.41 (1C, –OCH_3), 113.84 (2C, ArH), 121.85 (1C, C_α), 128.35 (2C, ArH), 128.95 (2C, ArH), 130.32 (1C, ArH), 130.80 (2C, ArH), 131.07 (1C, Ar), 135.06 (1C, Ar), 143.91 (1C, C_β), 163.42 (1C, $ArOCH_3$), 188.65 (1C, C=O).

Synthesis of 3-(4-hydroxyphenyl)-5-phenyl-4,5-dihydro-1*H*-pyrazole-1-carbaldehyde (Pyrazoline 1)

Pyrazolines **1-2** were synthesized based on literature (Wahyuningsih *et al*., 2019) with slight modifications. A mixture of 0.22 g (1 mmol) chalcone **1**, 0.5 mL (10 mmol) hydrazine hydrate, and 10 mL of 30% (w/v) NaOH in ethanol was added in a three-neck round bottom flask. The mixture was refluxed for 24 hours. Then, 5 mL of 98-100% formic acid was added dropwise, and the reflux was continued for 16 h. The reaction mixture was then cooled in the refrigerator for 48 hours until a precipitate formed. The precipitate was filtered, washed with cold aquadest, and dried under vacuum to obtain the product as an orange solid, yielding 41.35%, purity of 100% by GC-MS, and a melting point of 201 °C. Mass spectrum (EI), m/z: 266 (M^+). FTIR spectrum (KBr), ν_{max} (cm^{-1}): 3201 (O–H str.), 3032 (C_{sp2}–H str.), 1643 (C=O str.), 1604 (C=N str.), 1519 and 1442 (aromatic C=C str.), 1172 (C–N str.). ^{1}H-NMR (500 MHz), δ (ppm): 3.13 (1H, *dd*, J = 5, 18 Hz, CH_2 (H_A)), 3.85 (1H, *dd*, J = 11.5, 18 Hz, CH_2 (H_B)), 3.98 (1H, *dd*, J = 5, 11.5 Hz, CH (H_x)), 6.83 (2H, *d*, J = 8.5 Hz, ArH), 7.21 (2H, *d*, J = 7.5 Hz, ArH), 7.26 (1H, *t*, J = 7.5 Hz, ArH), 7.34 (2H, *t*, J = 7.5 Hz, ArH), 7.62 (2H, *d*, J = 9 Hz, ArH), 8.85 (1H, *s*, –CH=O), 10.07 (1H, *s*, O–H). ^{13}C-NMR (125 MHz), δ (ppm): 42.39 (1C, CH_2), 58.18 (1C, CH), 115.58 (2C, ArH), 121.60 (1C, ArH), 125.58 (2C, ArH), 127.38 (1C, Ar), 128.51 (2C, ArH), 128.67 (2C, ArH), 141.45 (1C, Ar), 156.02 (1C, C), 159.22 (1C, CH=O), 159.69 (1C, ArOH).

Synthesis of 3-(4-methoxyphenyl)-5-phenyl-4,5-dihydro-1*H*-pyrazole-1-carbaldehyde (Pyrazoline 2)

To synthesize pyrazoline **2**, the same procedure was used as for the synthesis of pyrazoline **1**, using 0.24 g (1 mmol) chalcone **2,** 0.5 mL (10 mmol) hydrazine hydrate, and 10 mL 30% (w/v) NaOH in ethanol. The product was obtained as a white solid with 53.57% yield, 100% purity by GC-MS, and a melting point at 125 °C. Mass spectrum (EI), m/z: 280 (M^+). FTIR spectrum (KBr), ν_{max} (cm^{-1}): 3024 (C_{sp2}–H str.), 2900 (C_{sp3}–H str.), 1681 (C=O str.), 1604 (C=N str.), 1520 and 1427 (aromatic C=C str.), 1257 (C–

O), 1172 (C–N str.). ^{1}H-NMR (500 MHz), δ (ppm): 3.18 (1H, *dd*, J = 4.5, 17.5 Hz, CH_2 (H_A)), 3.77 (1H, *dd*, J = 12, 17.5 Hz, CH_2 (H_B)), 3.84 (3H, *s*, OCH_3), 5.51 (1H, *dd*, J = 4.5, 12 Hz, CH (H_x)), 6.93 (2H, *d*, J = 9 Hz, ArH), 7.25 (1H, *t*, *J* = 6 Hz, ArH), 7.27 (2H, *d*, J = 7.5 Hz, ArH), 7.32 (2H, *t*, J = 7.5 Hz, ArH), 7.67 (2H, *d*, J = 9.5 Hz, ArH), 8.93 (1H, *s*, –CH=O). ^{13}C-NMR (125 MHz), δ (ppm): 42.80 (1C, CH_2), 55.5 (1C, OCH_3), 58.99 (1C, CH), 114.33 (2C, ArH), 123.60 (1C, ArH), 125.75 (2C, ArH), 128.02 (1C, Ar), 128.40 (2C, ArH), 129.09 (2C, ArH), 140.81 (1C, Ar), 155.57 (1C, C), 160.00 (1C, CH=O), 161.68 (1C, $ArOCH_3$).

Drug-likeness and ADMET Prediction

The drug-likeness properties of the pyrazolines **1-2** were predicted using Lipinski's rule of five. The parameters used were molecular weight, log P value, number of hydrogen bond acceptors, and number of hydrogen bond donors. These predictions were performed using an online-based program called SwissADME (Daina *et al*., 2017).

SwissADME was also used to predict the ADME profiles of pyrazolines **1-2**, including skin permeation value (log Kp), gastrointestinal (GI) absorption, blood-brain barrier (BBB) permeability, and probability interaction against P-gp substrate, CYP1A2, CYP2C19, CYP2C9, CYP2D6, and CYP3A4 inhibitors. Moreover, Pro-Tox II, an online-based program, was employed to predict the LD_{50} value, toxicity class, and various types of organ toxicity (Banerjee et. al., 2018).

Cytotoxicity Evaluation

The cytotoxicity evaluation was performed based on the literature (Tolosa *et al*., 2015) with some modifications. All cancer cell lines (WiDr, HeLa, MCF7, T47D, 4T1) and Vero cell lines were incubated for 24 h in 96-well plates at 37°C. The newly synthesized pyrazolines **1-2** were prepared in DMSO solution and diluted with culture medium solution to make a series of concentrations of 400; 200; 100; 50; 25; 12.5; 6.25; 3.125 μg/mL. Next, 100 μL of each concentration was added to each cell well and incubated for 24h under the same condition. Afterward, the plate's culture medium was removed, and MTT solution was added to the plates. The absorbance was measured using ELISA Reader at 595 nm. These results were used to determine the correlation between the compound concentration with the cell viability. The IC_{50} values of pyrazolines **1-2** against all tested cell lines were then determined using probit analysis, and the selectivity index (SI) values were calculated from the IC_{50} of pyrazolines **1-2** in normal cells compared to cancer cells.

Molecular Docking Study

The epidermal growth factor receptor tyrosine kinase (EGFR-TK) was used in the molecular docking study of pyrazolines **1-2** by AutoDock Vina (Trott & Olson, 2010). The three-dimensional structure of the receptor was obtained from Protein Data Bank (PDB ID: 4HJO) (Park *et al*., 2012) and was complexed with erlotinib as the native ligand. The preparation of the receptor was done using AutoDock Tools 1.5.6, whereas the structure of the pyrazolines **1-2** was modeled using GaussView and optimized using Gaussian09 (Frisch *et al*., 2016) based on the density functional theory (B3LYP/6-311G) method. The molecular docking protocol was validated by performing the redocking of erlotinib. Both redocking and docking were conducted in a grid box of 20 Å ×20 Å ×20 Å with a spacing of 1.00 Å. The most preferable conformation was selected based on the lowest binding affinity value. The docking results were visualized using Discovery Studio Visualizer 2020.

RESULTS AND DISCUSSION

The Synthesis

The reaction scheme for synthesizing 1-formyl-2-pyrazoline derivatives (Figure 1). First, chalcones **1-2** were synthesized through an aldol condensation reaction under ultrasonic irradiation with a slight modification of the method described in the literature (Suma *et al*., 2019). The use of montmorillonite as a heterogeneous catalyst increased the yield of chalcone **1** from 12.5% to 89.28%. The structure elucidation of chalcones **1-2** was conducted using several spectrometers. The mass spectra showed the ion molecular (M^+) fragment corresponding to the molecular weight of both chalcones. The IR spectra of both compounds exhibited the presence of C=O and *trans* C–H bonds, indicating the formation of chalcone. The ^{1}H-NMR spectra confirmed the presence of *trans* alkene protons, while the ^{13}C-NMR spectra showed the presence of the carbon atom in the carbonyl group.

Chalcones **1** and **2** were utilized to synthesize 1-formyl-2-pyrazoline derivatives by a cyclo-condensation reaction with hydrazine hydrate according to the literature method with a minor alteration of utilizing formic acid instead of acetic acid (Wahyuningsih *et al*., 2019). The mass spectra confirmed the molecular weight of the

newly synthesized pyrazolines **1-2** through the presence of the M^+ fragment. The formation of a pyrazoline ring was established by the IR spectra of both compounds, which exhibited the absence of *trans* C–H bonds and the presence of C–N and C=N bonds. Furthermore, the ^{1}H-NMR spectra revealed the pyrazoline ring formation by the absence of *trans* alkene protons and the presence of ABX proton systems of the three characteristic protons in the pyrazoline ring with a *doublet of doublet* splitting patterns (Suma *et al*., 2017). The ^{13}C-NMR spectra confirmed the number of carbon atoms in the desired pyrazolines.

Drug-likeness and ADMET Prediction

Adherence to Lipinski's Rule of Five is an important factor in identifying promising drug candidates during the earliest step of drug discovery and development. The rule highlights the significance of molecular properties in determining oral bioavailability, with the key parameters including molecular weight < 500 Da, log P value < 5, number of hydrogen bond acceptors < 10, and number of hydrogen bond donors < 5 (Bickerton *et al*., 2012). Pyrazolines **1** and **2** conform to the rule, as determined by the prediction results generated by SwissADME. Pyrazoline **1** ($C_{16}H_{14}N_2O_2$) has a molecular weight of 266, H-bond acceptors of 3, H-bond donor of 1, and a log P value of 2.22. While pyrazoline **2** ($C_{17}H_{16}N_2O_2$) has a molecular weight of 280, H-bond acceptors of 3, no H-bond donor, and a log P value of 2.62. This result indicates that they possess drug-like properties.

Adequate ADME properties are crucial for drug candidates. The ADME prediction results for pyrazolines **1** and **2** obtained from SwissADME (Table I) indicated that these compounds have favorable ADME properties. Both compounds have medium skin permeation, good absorption, high gastrointestinal (GI) absorption, and the ability to cross the blood-brain barrier (BBB). None of the synthesized compounds were predicted as P-glycoprotein substrates. It is reported that the inhibition of cytochromes P450 (CYP) isoenzymes is one major cause of pharmacokinetics-related drug-drug interactions leading to adverse effects due to the accumulation of the drug and/or its metabolites (Hollenberg, 2002). Pyrazoline **1** was predicted to be a non-inhibitor of all five enzymes, while pyrazoline **2** was predicted to be an inhibitor of CYP2C19 and CYP2C9.

Furthermore, the ideal drug candidates should not be toxic to the body. ProTox-II was used to predict the toxicity of pyrazoline **1** and **2** in a normal body condition (Table II). The prediction method classifies the toxicity into different levels, such as oral toxicity, organ toxicity (hepatotoxicity), and toxicological endpoints (carcinogenicity, immunotoxicity, mutagenicity, and cytotoxicity). Based on the predicted LD_{50} values, pyrazoline **1** was classified as a toxicity class 4 compound, while pyrazoline **2** was classified as a toxicity class 5 compound. In the ProTox-II webserver, these toxicity classes are defined according to the globally harmonized system of classification and labeling of chemicals (GHS). Compounds in class 4 with an LD_{50} value of 300-2000 mg/kg are said to be harmful if swallowed, while compounds in class 5 with an LD_{50} value of 2000-5000 mg/kg are said to may be harmful if swallowed (Banerjee *et al*., 2018). According to the prediction, both pyrazoline **1-2** were also inactive in immunotoxicity, mutagenicity, and cytotoxicity. Based on their drug-likeness and ADMET prediction results, both pyrazolines **1-2** have satisfactory properties and have the potential to be studied further as drug candidates.

The Cytotoxicity Evaluation against Cancer Cells

The anticancer activity study of pyrazolines **1-2** was performed by evaluating their cytotoxic properties using MTT assay against several cancer cell lines, i.e., WiDr (colorectal cancer), HeLa (cervical cancer), MCF7, T47D, and 4T1 (breast cancer). The toxicity was classified as potent (IC_{50} < 1 μM), strong (IC_{50} = 1-20 μM), moderate (IC_{50} = 20-100 μM), low (IC_{50} = 100-200 μM), and inactive (IC_{50} >200 μM) (Indrayanto *et al*., 2021). Pyrazoline **1** exhibited moderate activity with the highest cytotoxicity against Hela cancer cells (IC_{50} = 25.01 μM) and low activity against WiDr, MCF7, T47D, and 4T1 cancer cells (Table III). On the other hand, pyrazoline **2** displayed moderate cytotoxic activity against MCF7 and 4T1 cancer cells (IC_{50} = 82.87 and 92.70 μM), but was inactive against WiDr, HeLa, and T47D cancer cells.

Evaluation of the Selectivity Index (SI) value is also crucial in determining the feasibility of further work on a compound's anticancer activity. To calculate the SI value, the cytotoxicity of the compound against non-malignant cell lines must be determined. In this study, Vero cell lines were used as non-malignant cells. An SI value of ≥3 is required to classify a compound as a prospective anticancer agent (Weerapreeyakul *et al*., 2012).

Table I. The result of ADME prediction

Compd	Skin permeation value (log Kp) (cm/s)	GI absorption	BBB permeability	P-gp substrate	Inhibitor interaction				
					CYP1A2	CYP2C19	CYP2C9	CYP2D6	CYP3A4
1	-6.25	High	Yes	No	No	No	No	No	No
2	-6.10	High	Yes	No	No	Yes	Yes	No	No

Table II. The result of toxicity prediction in normal condition

Compd	LD_{50} (mg/kg)	Toxicity class	Hepatotoxic	Toxicological Endpoints			
				Carcinogenic	Immunotoxic	Mutagenic	Cytotoxic
1	1880	4	Active	Active	Inactive	Inactive	Inactive
2	2500	5	Active	Active	Inactive	Inactive	Inactive

Table III. The result of the cytotoxicity evaluation on cancer cells

Cells	IC_{50} value (μM)		Selectivity Index	
	Pyrazoline 1	Pyrazoline 2	Pyrazoline 1	Pyrazoline 2
WiDr	144.58	>200	1.54	2.78
HeLa	25.01	>200	8.92	3.67
MCF7	121.60	82.87	1.84	14.45
T47D	155.30	>200	1.44	0.20
4T1	134.90	92.70	1.65	12.92
Vero (non-malignant)	223.12	1197.29	-	-

Table IV. The result of molecular docking

Compound	Binding affinity (kcal/mol)	H-Bond	Other Interactions				
			Hydrophobic	Van der Waals	Electrostatic	C-H bond	Pi-Sulphur
Erlotinib	-7.1 (RMSD 1.014 Å)	Met769	Lys721, Val702, Ala719, Leu694, Leu820	Asp831, Thr830, Cys773, Asp776, Phe771, Pro770, Gly772, Leu768 Ile720, Ile765, Thr766	-	Leu764, Gln767, Met769	-
Pyrazoline 1	-7.9	Lys721, Leu764	Lys721, Val702, Ala719	Asp831, Thr830, Ile720, Ile765, Thr766, Leu820, Leu694, Gly695	-	-	Cys773
Pyrazoline 2	-8.0	Lys721	Lys721, Val702, Leu820, Leu694, Leu753, Leu834, Leu764	Asp831, Thr830, Cys773, Thr766,	-	-	-

The calculated SI values for pyrazolines **1-2** (Table III). Pyrazoline **1** exhibited good selectivity for HeLa cells, while pyrazoline **2** demonstrated good selectivity for HeLa, MCF7, and 4T1 cells.

The results suggest that pyrazoline **1** could be further investigated as a potential anticancer agent for cervical cancer, particularly against HeLa cells, due to its moderate IC_{50} value and good selectivity. On the other hand, pyrazoline **2** could be a promising candidate for breast cancer treatment, particularly against MCF7 cancer cells, due to its moderate IC_{50} value and high selectivity index.

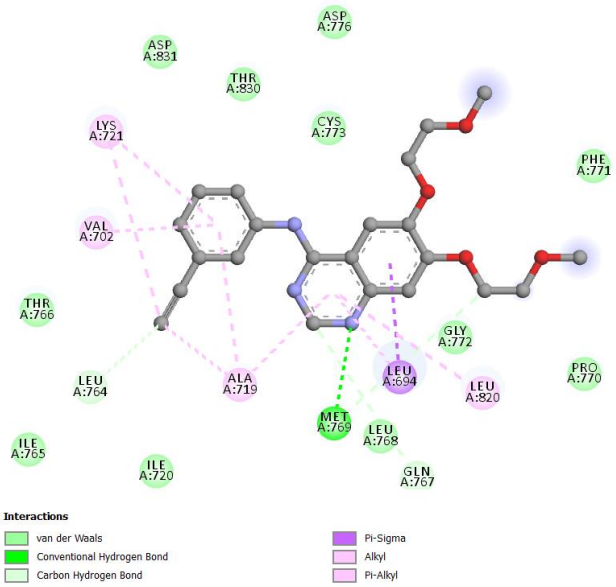

(a)

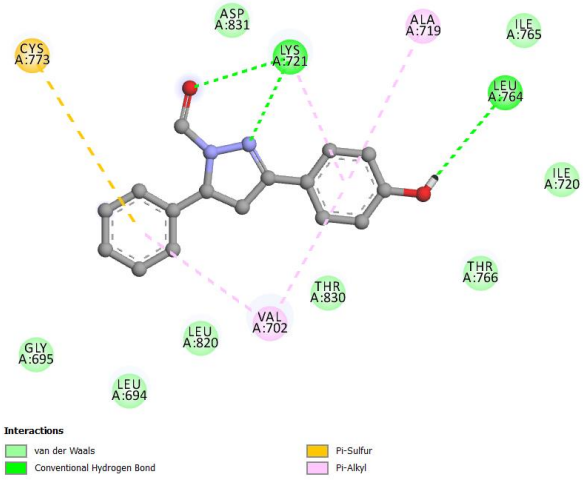

(b)

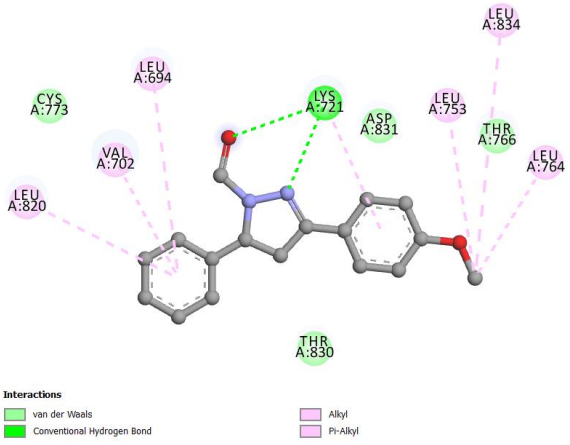

(c)

Figure 2. The binding interaction of (a) Erlotinib, (b) Pyrazoline 1, (c) Pyrazoline 2 against EGFR-TK (PDB ID: 4HJO)

Molecular Docking Study

A molecular docking study was conducted using EGFR-TK (PDB ID: 4HJO) as the target protein. EGFR-TK was selected due to its significant role in developing and growing various types of tumors (Mitsudomi & Yatabe, 2010). This study aimed to investigate the binding modes of pyrazoline **1-2** with EGFR-TK and compare them with those of erlotinib, the native ligand (Table IV).

The redocking of EGFR-TK with its native ligand showed that erlotinib was stable enough to attach to the binding site with a binding affinity value of -7.1 kcal/mol. The root mean square deviation (RMSD) value was 1.014 Å. The value was lower than 2 Å, indicating that the docking was valid (Ramírez & Caballero, 2018). The docking resulted in the formation of hydrogen bonds on Met769 residue, hydrophobic interaction on Lys721, Val702, Ala719, Leu694, and Leu820 residue, Van der Waals interaction, and carbon-hydrogen bond interaction on several amino acid residues. Among these interactions, hydrophobic interaction on Lys721 residue is essential for ATP binding in the EGFR kinase domain, and the subsequent phosphorylation of tyrosine amino acids on proteins such as PI-3-kinase (K), phospholipase C, and the EGFR (Li *et al*., 2003). Therefore, inhibitors such as erlotinib block the catalytic site of EGFR, preventing the binding of ATP and hence suppressing its intrinsic protein kinase activity. Based on the 2D visualization of the interaction between erlotinib and EGFR-TK (Figure 2) it can be seen that erlotinib had hydrophobic interaction with Lys721 residue via its aromatic ring.

The synthesized pyrazolines **1** and **2** had a higher binding affinity in the binding site of EGFR-TK compared to erlotinib with the values of -7.9 and -8.0 kcal/mol, respectively. Compared to erlotinib, both pyrazolines exhibited similar interactions with EGFR-TK, such as hydrogen bonds, hydrophobic, and Van der Waals interactions, demonstrating their ability to bind to EGFR-TK. Moreover, pyrazolines **1-2** interacted with Lys721 residue, indicating their ability to block the catalytic site of EGFR-TK, inhibiting cancer cell growth by preventing ATP from binding. Pyrazolines **1-2** exhibited two possible interactions, namely hydrogen bonds and hydrophobic interaction, while erlotinib only exhibited hydrophobic interaction. The presence of the pyrazoline ring and formyl group were crucial factors in enhancing the anticancer activity of the compound, as evidenced by the additional interactions of hydrogen bonds between the pyrazolines ring nitrogen and formyl group oxygen with the Lys721 residue (Figure 2b, 2c). Moreover, the hydroxy substituent in pyrazoline **1** and the methoxy substituent in pyrazoline **2** contributed to their anticancer activity by interacting with several amino acid residues via hydrogen bond and hydrophobic interaction, respectively.

CONCLUSION

We have designed, synthesized, and evaluated the bioactivity of two novel 1-formyl-2-pyrazoline derivatives. Both compounds demonstrated promising results as anticancer in terms of their drug-likeness and ADMET properties, cytotoxic activity against HeLa and MCF7 cancer cells, and interaction with the EGFR-TK receptor. This result suggests that both compounds can be considered potential lead compounds for anticancer candidates. However, additional investigation and evaluation are needed for further development as clinical anticancer therapeutics.

ACKNOWLEDGMENT

The financial support for this study from the Faculty of Pharmacy, Universitas Gadjah Mada through the "Hibah Penelitian Dosen Muda" program in the year 2023 is greatly acknowledged and appreciated.

CONFLICT OF INTEREST

The authors declare no conflict of interest associated with this work.

REFERENCES

Banerjee, P., Eckert, A. O., Schrey, A. K., & Preissner, R. (2018). ProTox-II: a webserver for the prediction of toxicity of chemicals. *Nucleic Acids Research*, *46*(W1), W257–W263. https://doi.org/10.1093/nar/gky318

Bickerton, G. R., Paolini, G. V., Besnard, J., Muresan, S., & Hopkins, A. L. (2012). Quantifying the chemical beauty of drugs. *Nature Chemistry*, *4*(2), 90–98. https://doi.org/10.1038/nchem.1243

Brennan, P., & Davey-Smith, G. (2022). Identifying novel causes of cancers to enhance cancer prevention: new strategies are needed. *Journal of the National Cancer Institute*, *114*(3), 353–360. https://doi.org/10.1093/jnci/djab204

Daina, A., Michielin, O., & Zoete, V. (2017). SwissADME: a free web tool to evaluate

pharmacokinetics, drug-likeness and medicinal chemistry friendliness of small molecules. *Scientific Reports*, *7,* 42717. https://doi.org/10.1038/srep42717

Frisch, M. J., Trucks, G. W., Schlegel, H. B., Scuseria, G. E., Robb, M. A., Cheeseman, J. R., Scalmani, G., Barone, V., Petersson, G. A., Nakatsuji, H., Li, X., Caricato, M., Marenich, A. V., Bloino, J., Janesko, B. G., Gomperts, R., Mennucci, B., Hratchian, H. P., Ortiz, J. V., Izmaylov, A. F., Sonnenberg, J. L., Williams-Young, D., Ding, F., Lipparini, F., Egidi, F., Goings, J., Peng, B., Petrone, A., Henderson, T., Ranasinghe, D., Zakrzewski, V. G., Gao, J., Rega, N., Zheng, G., Liang, W., Hada, M., Ehara, M., Toyota, K., Fukuda, R., Hasegawa, J., Ishida, M., Nakajima, T., Honda, Y., Kitao, O., Nakai, H., Vreven, T., Throssell, K., Montgomery, J. A., Jr., Peralta, J. E., Ogliaro, F., Bearpark, M. J., Heyd, J. J., Brothers, E. N., Kudin, K. N., Staroverov, V. N., Keith, T. A., Kobayashi, R., Normand, J., Raghavachari, K., Rendell, A. P., Burant, J. C., Iyengar, S. S., Tomasi, J., Cossi, M., Millam, J. M., Klene, M., Adamo, C., Cammi, R., Ochterski, J. W., Martin, R. L., Morokuma, K., Farkas, O., Foresman, J. B., & Fox, D. J. (2016). Gaussian, Inc., Wallingford CT.

Haider, K., Shafeeque, M., Yahya, S., & Yar, M. S. (2022). A comprehensive review on pyrazoline based heterocyclic hybrids as potent anticancer agents. *European Journal of Medicinal Chemistry Reports*, *5*, 100042. https://doi.org/10.1016/J.EJMCR.2022.100042

Hollenberg, P. F. (2002). Characteristics and common properties of inhibitors, inducers, and activators of CYP enzymes. *Drug Metabolism Reviews, 34*(1&2), 17-35. https://doi.org/10.1081/dmr-120001387

Indrayanto, G., Putra, G. S., & Suhud, F. (2021). Validation of *in-vitro* bioassay methods: Application in herbal drug research. In *Profiles of Drug Substances, Excipients, and Related Methodology*, *46*, (pp. 273–307). https://doi.org/10.1016/bs.podrm.2020.07.005

Joshi, G., Sharma, M., Kalra, S., Gavande, N. S., Singh, S., & Kumar, R. (2021). Design, synthesis, biological evaluation of 3,5-diaryl-4,5-dihydro-1H-pyrazole carbaldehydes as non-purine xanthine oxidase inhibitors: Tracing the anticancer mechanism via xanthine oxidase inhibition. *Bioorganic Chemistry*, *107*. https://doi.org/10.1016/j.bioorg.2020.104620

Karabacak, M., Altıntop, M. D., Çiftçi, H. İ, Koga, R., Otsuka, M., Fujita, M., & Özdemir, A. (2015). Synthesis and evaluation of new pyrazoline derivatives as potential anticancer agents. *Molecules*, *20*, 19066-19084. https://doi.org/10.3390/molecules201019066

Lang, D., Kaur, R., Arora, R., Saini, B., & Arora, S. (2020). Nitrogen-containing heterocycles as anticancer agents: an overview. *Anti-Cancer Agents in Medicinal Chemistry, 20*(18), 2150-2168. https://doi.org/10.2174/1871520620666200705214917

Li, J., Ma, C., Huang, Y., Luo, J., & Huang, C. (2003). Differential requirement of EGF receptor and its tyrosine kinase for AP-1 transactivation induced by EGF and TPA. *Oncogene*, *22*(2), 211–219. https://doi.org/10.1038/sj.onc.1206102

Matiadis, D. (2023). Strategies and methods for the synthesis of 2-pyrazolines: recent developments (2012–2022). *Advanced Synthesis and Catalysis*, *365*, 1934-1969. https://doi.org/10.1002/adsc.202300373

Matiadis, D., & Sagnou, M. (2020). Pyrazoline hybrids as promising anticancer agents: an up-to-date overview. *International Journal of Molecular Sciences*, *21*(15), 5507. https://doi.org/10.3390/ijms21155507

Mitsudomi, T., & Yatabe, Y. (2010). Epidermal growth factor receptor in relation to tumor development: EGFR gene and cancer. *The FEBS Journal, 277*(2), 301–308. https://doi.org/10.1111/j.1742-4658.2009.07448.x

Mustofa, Satriyo, P. B., Suma, A. A. T., Waskitha, S. S. W., Wahyuningsih, T. D., & Sholikhah, E. N. (2022). A potent EGFR inhibitor, N-phenyl pyrazoline derivative suppresses aggressiveness and cancer stem cell-like phenotype of cervical cancer cells. *Drug Design, Development and Therapy*, *16*, 2325–2339. https://doi.org/10.2147/DDDT.S350913

Nehra, B., Rulhania, S., Jaswal, S., Kumar, B., Singh, G., & Monga, V. (2020). Recent advancements in the development of bioactive pyrazoline derivatives. *European Journal of Medicinal Chemistry*, *205*, 112666. https://doi.org/10.1016/j.ejmech.2020.112666

Park, J. H., Liu, Y., Lemmon, M. A., & Radhakrishnan, R. (2012). Erlotinib binds both inactive and active conformations of the EGFR tyrosine kinase domain. *Biochemical Journal*, *448*(3), 417–423. https://doi.org/10.1042/BJ20121513

Ramírez, D., & Caballero, J. (2018). Is it reliable to take the molecular docking top scoring position as the best solution without considering available structural data? *Molecules*, *23*(5), 1038. https://doi.org/10.3390/molecules23051038

Rana, M., Faizan, M. I., Dar, S. H., Ahmad, T., & Rahisuddin. (2022). Design and Synthesis of Carbothioamide/Carboxamide-Based Pyrazoline Analogs as Potential Anticancer Agents: Apoptosis, Molecular Docking, ADME Assay, and DNA Binding Studies. *ACS Omega*, *7*(26), 22639–22656. https://doi.org/10.1021/acsomega.2c02033

Rashid, M., Afzal, O., & Altamimi, A. S. A. (2021). Benzimidazole molecule hybrid with oxadiazole ring as antiproliferative agents: in-silico analysis, synthesis and biological evaluation. *Journal of the Chilean Chemical Society,* *66*(2), 5164-5182. http://dx.doi.org/10.4067/S0717-97072021000205164

Suma, A. A. T., Wahyuningsih, T. D., & Mustofa. (2019). Synthesis, cytotoxicity evaluation and molecular docking study of *N*-phenylpyrazoline derivatives. *Indonesian Journal of Chemistry*, *19*(4), 1081–1090. https://doi.org/10.22146/ijc.45777

Suma, A. A. T., Wahyuningsih, T. D., & Pranowo, D. (2017). Synthesis and antibacterial activities of N-phenylpyrazolines from veratraldehyde. *Materials Science Forum*, *901*, 124–132. https://doi.org/10.4028/www.scientific.net/MSF.901.124

Sung, H., Ferlay, J., Siegel, R. L., Laversanne, M., Soerjomataram, I., Jemal, A., & Bray, F. (2021). Global cancer statistics 2020: GLOBOCAN estimates of incidence and mortality worldwide for 36 cancers in 185 countries. *CA: A Cancer Journal for Clinicians*, *71*(3), 209–249. https://doi.org/10.3322/caac.21660

Tolosa, L., Donato, M. T., & Gómez-Lechón, M. J. (2015). General cytotoxicity assessment by means of the MTT assay. *Methods in Molecular Biology*, *1250,* 333–348. https://doi.org/10.1007/978-1-4939-2074-7_26

Trott, O., & Olson, A. J. (2010). AutoDock Vina: Improving the speed and accuracy of docking with a new scoring function, efficient optimization, and multithreading. *Journal of Computational Chemistry*, *31*, 455-461. https://doi.org/10.1002/jcc.21334

Upadhyay, A. (2021). Cancer: an unknown territory; rethinking before going ahead. In *Genes and Diseases*, *8*(5), 655–661. https://doi.org/10.1016/j.gendis.2020.09.002

Vahedpour, T., Hamzeh-Mivehroud, M., Hemmati, S., & Dastmalchi, S. (2021). Synthesis of 2-pyrazolines from hydrazines: Mechanisms explained. *ChemistrySelect*, *6*(25), 6483–6506. https://doi.org/10.1002/slct.202101467

Wahyuningsih, T. D., Suma, A. A. T., & Astuti, E. (2019). Synthesis, anticancer activity, and docking study of N-acetyl pyrazolines from veratraldehyde. *Journal of Applied Pharmaceutical Science*, *9*(3), 14–20. https://doi.org/10.7324/JAPS.2019.90303

Weerapreeyakul, N., Nonpunya, A., Barusrux, S., Thitimetharoch, T., & Sripanidkulchai, B. (2012). Evaluation of the anticancer potential of six herbs against a hepatoma cell line. *Chinese Medicine*, *7*(1), 15. https://doi.org/10.1186/1749-8546-7-15

Zhong, L., Li, Y., Xiong, L., Wang, W., Wu, M., Yuan, T., Yang, W., Tian, C., Miao, Z., Wang, T., & Yang, S. (2021). Small molecules in targeted cancer therapy: advances, challenges, and future perspectives. *Signal Transduction and Targeted Therapy*, 6, 201. https://doi.org/10.1038/s41392-021-00572-w